High-Precision Spectrographs for Exoplanet Research: CORAVEL, ELODIE, CORALIE, SOPHIE, and HARPS

40

Francesco Pepe, François Bouchy, Michel Mayor, and Stéphane Udry

Contents

F. Pepe (✉)
Département d'Astronomie, Observatoire de l'Université de Genéve, Versoix, GE, Switzerland
e-mail: Francesco.Pepe@unige.ch

F. Bouchy
Département d'Astronomie, Université de Genéve, Versoix, GE, Switzerland

Observatoire astronomique de l'Université de Genéve, Versoix, Switzerland

LAM/OHP, Marseille, France
e-mail: Francois.Bouchy@unige.ch

M. Mayor · S. Udry
Département d'Astronomie, Université de Genéve, Versoix, GE, Switzerland
e-mail: Michel.Mayor@unige.ch; Stephane.Udry@unige.ch

H. J. Deeg, J. A. Belmonte (eds.), *Handbook of Exoplanets*,
https://doi.org/10.1007/978-3-319-55333-7_190

Abstract

In this chapter, we will present the concepts, designs, and performances of several generations of simultaneous-reference spectrographs that have made the history of exoplanet discoveries by means of the Doppler technique. It is not possible to understand the strengths of this category of spectrographs without understanding first the revolutionary approach of CORAVEL that set the path for the next generation of instruments using CCDs, i.e., ELODIE and CORALIE. These instruments were extremely successful (e.g., with the discovery of 51 Peg b), it however quickly became clear that higher precision would be necessary in order not to remain stuck with Jupiter- and Saturn-mass planets only. The ELODIE/CORALIE concept was optimized in order to reach best possible performances. This process led to the development of HARPS that has become, through the tens of discoveries of Super-Earths and Neptunes, the new reference for high-precision Doppler velocity measurements. The success of HARPS had to be transposed to the northern hemisphere, an ambition that resulted first in the manufacturing of SOPHIE and later of HARPS-N. This work was finally the baseline for the development of ESPRESSO aiming at the next level of precision. We refer, however, to the chapter dedicated to ESPRESSO in this same handbook for a detailed description.

Introduction

The pace of early history of exoplanet discoveries was dictated by the Doppler (or Radial-Velocity) technique. A review of past, present, and future spectrographs dedicated to the search for exoplanets is given by Pepe et al. (2014). The successful spectrographs, although of quite different design, can be split into two major categories: The "self-calibrated" and the "simultaneous reference" spectrographs. In the present chapter, we shall focus on this second category. Its concept is based on the ability of a stable spectrograph to measure in the most direct way a spectral line position on the detector, convert it into wavelength, and determine the radial-velocity of the astrophysical object by comparing the measured wavelength with the rest-frame wavelength in the solar barycenter. When aiming at ms^{-1} precision, the motion of the spectral line in the focal plane of the spectrograph becomes so tiny that it is actually comparable or eventually much smaller than any physical motion of the detector with regard to the spectrum. A method must, therefore, be introduced, in addition to the initial wavelength calibration, to track these instrumental drifts. In the case of the "simultaneous reference" technique, this objective is achieved by projecting, at any time, a laboratory reference spectrum (usually a spectral standard) into the focal/spectral plane simultaneously with the calibration or the astrophysical spectrum. This allows to measure possible motions of the focal plane with regard to the detector and determine instrumental drifts, which can eventually be "subtracted" from the radial-velocity measurement.

In the following sections, we present several generations of "simultaneous-reference spectrographs." They are all based on the original CORAVEL concept, which will be introduced in order to develop the historical understanding of the instrumental evolution. We will then describe ELODIE – by which 51 Peg b (Mayor and Queloz 1995) was discovered – and its twin spectrograph CORALIE. We won't miss the occasion to describe the HARPS(−N) spectrograph, which has been crucial in triggering the era of "super-Earths" discoveries, as well as SOPHIE as its extension to the northern hemisphere. It is important to note that these spectrographs have contributed to a significant fraction of exoplanet discoveries (about 400 in total to date). The various sections will therefore also mention examples of the most important achievements of these spectrographs.

CORAVEL: The Beginning of Spectrovelocimetry

Historical Background

In a stellar spectrum, the Doppler information is distributed over several thousand of spectral lines. A large number of absorption lines are present over a broad spectral domain for the star of different spectral types, although some differences occur with varying atmospheric parameters. Felgett (1953) was first to suggest an instrumental setup to concentrate all this information into a single "signal" in order to extract the Doppler information: It would be "sufficient" to project the stellar spectrum on a physical binary mask/template to produce a cross-correlation signal that would achieve a minimum whenever the absorption lines would match the "holes" in the binary template. The transmitted signal is recorded as a function of the template position by a single detector. The so-obtained cross-correlation function (CCF) reproduces the "average" absorption line and its minimum will occur for the template position corresponding to the radial velocity of the star.

A first Coudé instrument (Griffin 1967) demonstrated the feasibility and huge efficiency of this approach compared to the classical radial-velocity measurements using photographic plates. An evolution of this concept was achieved with CORAVEL (Baranne et al. 1979, Fig. 1, Table 1). It is a cross-correlation spectrometer with two significant improvements: On the one hand, a compact cross-dispersed spectrograph using an echelle grating that allowed to cover a much larger spectral domain at high spectral resolution;on the other hand, a fully automatic control of the template scanning and a real-time access to the cross-correlation function and thus to the stellar radial velocity. If the position of the CCF allows for an efficient determination of the stellar radial velocity, the CCF itself permits the estimation of several other observables as well. For example, the area of the CCF (i.e., its equivalent width) at a given stellar temperature is a superb estimator of the metallicity of the observed star (Mayor 1980), a method broadly used with all subsequent cross-correlation spectrometers. The width of the CCF is furthermore a precise proxy for the stellar rotation (Benz and Mayor 1981, 1984).

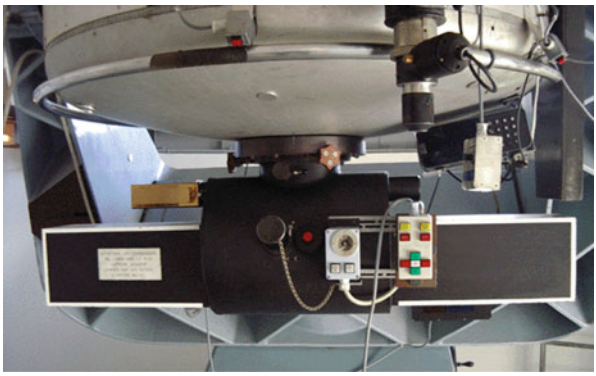

Fig. 1 The CORAVEL instrument at the Cassegrain focus of the 1-m Swiss Telescope at Observatoire de Haute-Provence (OHP)

Table 1 Main characteristics of CORAVEL

Parameters	Specification	Comments
Telescope	1-m class	CORAVEL-N was installed at the Cassegrain focus of the 1-m Swiss telescope at the Haute-Provence Observatory (1977); CORAVEL-S was installed at the Cassegrain focus of the 1.5 m Danish telescope at the ESO-La Silla Observatory (1981)
Feed	Slit spectrograph	
Design	Cross-dispersed echelle spectrograph	
Detector	Photomultiplier tube + physical mask	
Spectral domain	360–520 nm	
Resolving power R	20′000	
Efficiency	NA	
RV precision	300 m s^{-1}	

Results, Precision Limitations, Lessons Learned

CORAVEL has been a revolutionary instrument in terms of stellar physics, kinematics, and the exploration of binary systems. In this chapter, it has been described, however, as the precursor of future spectrographs optimized for and dedicated to the search of extrasolar planets through precise Doppler measurements rather than an instrument that contributed to the development of the exoplanet science in a direct way. Nevertheless, it must be recalled that CORAVEL allowed (in combination with Oak Ridge measurements) for the determination of the orbit of the companion of HD 114762 (Latham et al. 1989), a companion that has a minimum mass of 11 M_J at the interface between giant planets and brown dwarfs. According to the planet-mass distribution known today and depending on its actual mass, HD 114762 b could be considered as the first planetary companion to a solar-type star.

CORAVEL certainly had the capability of detecting high-mass exoplanets on short periods in the tail of the planet-mass distribution known today. However, before the discovery of the surprising properties of the population of giant gaseous planets, high-mass exoplanets were not expected (limited accretion of gas on a forming giant planet) and, moreover, we know now that these objects seem to be actually rare (decreasing distribution of the mass function towards high masses). Adding to this the limit of the radial-velocity observations allowing only for the estimate of a minimum mass for the companion, exoplanets were not the primary targets for CORAVEL.

CORAVEL had two main instrumental limitations that prevented radial-velocity measurements to be more precise than 300 ms^{-1}. First, it is a slit spectrometer; sub-arcsec errors on guiding translate in the most direct way into radial-velocity errors at the level of a fraction of km s^{-1}. Second, the built-in physical template and the observed stellar spectrum do not always perfectly match, especially considering varying temperature and air pressure of the spectrograph, that furthermore was not of the stabilized type. With the advent of CCDs and optical fibers, new opportunities appeared to remove these limitations. The era of a new generation of spectrovelocimeters was about to start.

ELODIE and CORALIE: Planet Discovery by Numerical Cross-Correlation

Technical Improvements

The success of the two CORAVEL instruments has clearly demonstrated that the cross-correlation approach was providing an efficient way of extracting the Doppler information from stellar spectra. Also, as mentioned in the previous section, the limitations of the instruments were fairly well understood and new technology developments allowed for the design of new instruments based on the same basic principles for precise velocity measurements while incorporating these new features.

CCD detectors and numerical cross-correlation. With CORAVEL, the cross-correlation between the stellar spectrum and a binary mask was performed mechanically within the instrument, sweeping at high frequency through a predefined set of mask "positions" (channels), building in this way the CCF in real time by measuring the integrated counts in each of the visited channels using a photomultiplier. A major improvement of this approach was possible thanks to the advent of Charge-Coupled Device (CCD) detectors. It was then possible to record the stellar spectrum on the CCD and then perform the cross-correlation numerically, in a subsequent stage. The so-recorded spectra can also be used for spectroscopic analysis and the estimate of important stellar parameters (effective temperature, gravity, metallicity, individual element abundances, etc.).

Concerning the measurement of precise radial velocities, the new approach gives the possibility to use optimal numerical templates for the correlation, matching better the spectra of the stars observed. The single physical template in

CORAVEL was built from the spectrum of Arcturus, a giant K1.5 star. The measurement efficiency on stars of different spectral types (effective temperatures) decreases with increasing mismatch between the stellar spectrum and the numerical template (different sets and of spectral lines and different widths and depths). That was, e.g., a clear limit for M dwarfs, in addition to their intrinsic faintness.

The use of CCDs also pushed for the development of spectrographs at higher spectral resolution. At a resolving power of $R = 20{,}000$ (CORAVEL), many stellar spectral lines are blended due to instrumental broadening. An increase in resolving power allows for a better separation of the lines and a better determination of their position on the CCD due to better sampling and reduced photonic error (see also the section "HARPS: Setting New Standards").

Optical fibers. Another severe limitation of CORAVEL was the use of a slit at the entrance of the spectrograph. Due to atmospheric turbulence, seeing conditions, and varying telescope-instrument flexures, the image of the star on the entrance slit moves and results in a motion of the photocenter of the monochromatic slit image in the focal plane of the spectrograph. The observed shift directly translates into a shift of the stellar spectrum on the detector, mixing up spatial displacement and spectral shift (e.g., due to the Doppler effect). The shift on the CCD will change from one exposure to the next and introduce so a variation of the measured radial velocity up to hundreds of ms^{-1}. The use of optical fibers to feed the instrument allows, thanks to their scrambling effect, to produce a uniform and stable illumination of the spectrograph slit, increasing so the photocenter stability of the spectral lines on the detector to the level of a few ms^{-1}. However, optical fibers scramble only the near-field to a satisfactory level, while the far-field is left almost unchanged. In order to increase the scrambling effect even further, a double-scrambler device is therefore often introduced (Brown 1990). The double scrambler is composed of two fiber sections linked together by an optical device exchanging near- and far-field, thus ensuring that the second fiber scrambles the original (unscrambled) far-field of the first fiber section.

Calibration and stability. In order to achieve precise radial-velocity measurements, an important issue is to develop a calibration system allowing for the determination of the *zero velocity point* of the instrument for each measurement, reliable over long periods of time. With CORAVEL, this velocity calibration was obtained by the measurements of a hollow cathode iron lamp before and after the observation of a star. The interpolation between the zero velocities of the two measurements of the lamp gives then the position of the zero at the time of the star observation. Importantly, the measurement of the spectrum of the lamp allows as well for the determination of the wavelength calibration, i.e., the correspondence between the pixel and wavelength positions.

This approach is not sufficient anymore when aiming at high-precision radial velocities. Changes of the local astroclimatic conditions will induce spectral shifts on the CCD, mainly due to changes of the refraction index in the spectrograph. The local astroclimatic conditions impact as well the instrumental profile (IP) of the spectrograph, i.e., the way the photoelectrons of a line are distributed over the

CCD pixels, and thus the estimated radial velocity. Two different methods have been developed to overcome this difficulty:

- *Self-calibration:* The visible light from the star is passing through a gas cell (historically HF, later I_2) whose absorption spectrum is then superimposed to the stellar one, providing a built-in reference wavelength calibration and radial-velocity measurement (Campbell and Walker 1979; Brown 1990; Butler et al. 1996). This approach is perfectly adapted to existing (nonstabilized) echelle spectrographs directly mounted to the telescope. Any distortion, drift, thermo-mechanical and optical effect, etc. will affect the IP of the spectrograph such that both stellar spectrum and spectral reference will "see" the same changes. In principle, it is possible to remove perfectly instrumental effects on the stellar spectrum by measuring the IP on the spectral reference. In practice, however, the limited wavelength range covered by the gas spectrum, its absorption, and the deconvolution process will significantly reduce the optical efficiency of the method. Furthermore, nonperfect knowledge of the high-resolution spectra of the spectral reference and the reference-free stellar spectrum may introduce systematic effects at the ms^{-1}-level.pag \enlargethispage*{-6pt}?>
- *Simultaneous reference:* Building on a stabilized spectrograph, the goal is to avoid as much as possible instrumental drifts and IP variations that may impact the stellar spectrum. Since, however, this can not be guaranteed at the level of millipixels on all timescales, a way is developed to track the residual instrumental drifts. For this purpose, two fibers feed the spectrograph simultaneously, one carrying the light of the observed star and the other the light from the spectral reference, usually a Thorium-Argon lamp (Brown 1990; Baranne et al. 1996). The two fibers at the entrance of the spectrograph are located as close together as possible to ensure almost identical optical path for both light beams, and they are organized such to produce on the CCD detector a series of interlaced spectral orders, the orders n of the lamp located in-between orders *n* and *n*-1 of the stellar spectrum, and vice versa (Fig. 2). The previously determined (typically

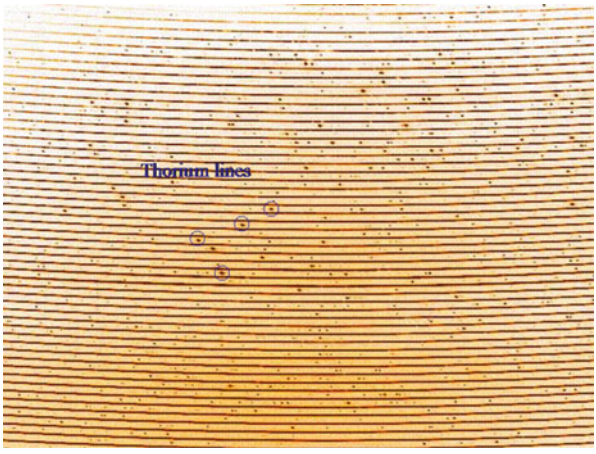

Fig. 2 Raw frame of a simultaneous-reference exposure showing the spectral orders of the stellar spectrum (horizontal lines) interlaced with the thorium-argon lamp spectrum (individual emission lines)

at the start of the night) wavelength solution that links together the wavelength with the pixel coordinate can be corrected, before being applied to the scientific observation, by the drift value determined by the shift of the reference spectrum between the calibration exposure and the scientific exposure. The advantages of this solution are that the optical throughput is conserved over the entire wavelength range and that complex deconvolution techniques are avoided. The disadvantage consists in the fact that the spectrograph must be conceived, right from the beginning, to be fiber-fed and as stable as possible, in order to avoid second-order instrumental effects. The method can therefore not be applied to any spectrograph.

The ELODIE and CORALIE Sisters

The ELODIE spectrometer (also known as "Super-Coravel") was considered in 1988 as a CORAVEL-derived instrument that would use available time of the 1.93-m telescope of Observatoire de Haute-Provence (OHP) during a full moon. ELODIE rapidly became one of the centerpieces of OHP in the 1990s. Designed by the OHP technical services in collaboration with André Baranne of the Observatoire de Marseille and with Michel Mayor of the Geneva Observatory, it was assembled in a laboratory and then tested on the sky in 1993. ELODIE was a fiber-fed cross-dispersed echelle spectrograph and was located in a temperature-controlled room in the first floor of the 1.93-m telescope building and covered with a double protection to improve its thermal stability. It was connected to the telescope by 20 m of a pair of optical fibers, from the front-end attached to the Cassegrain focus of the 1.93 m telescope. Two focal-plane apertures were available (both 2 arc-sec wide), one of which was used for starlight and the other for either the sky background or the wavelength calibration lamp, but could also be masked. The spectrograph used a 420×100 mm R4 echelle grating. The optical design was based on an asymmetric white-pupil mount, which allowed controlling the collimated beam size. In particular, the asymmetric design reduced the cross-disperser and camera-lens dimensions, therefore keeping the instrument compact and relatively cheap. The spectra covered a 3000 Å wavelength range (3850–6800 Å) with a spectral resolution of $R = 42{,}000$. The instrument was entirely computer-controlled and a standard data-reduction pipeline automatically processed the data from CCD readout, through extraction and wavelength calibration, to numerical cross-correlation and radial-velocity determination. The instrument is described in details by Baranne et al. (1996) and its characteristics are summarized in Table 2.

The first ELODIE spectrum was taken on June 1, 1993, during the period of testing which lasted until the end of 1993. The instrument was opened to the community in May 1994. It was with ELODIE that the first planet around a star other than the Sun was discovered around 51 Pegasi (Mayor and Queloz 1995). ELODIE worked until August 10, 2006, when its detector controller electronics broke down. It was quickly replaced by SOPHIE, then in its final phase of integration. ELODIE is today exposed and visible to visitors on the ground floor of the 1.93-m building at OHP (Fig. 3).

Table 2 Main characteristics of ELODIE/CORALIE

Parameters	Specification	Comments
Telescope	1–2 m class	ELODIE was installed on the 1.93-m telescope at the Haute-Provence Observatory (1994); CORALIE was installed on the 1.2-m Swiss Euler telescope at the ESO-La Silla Observatory (1998)
Feed	Fiber-fed spectrograph	Equipped with a double scrambler later on. CORALIE was equipped with octagonal fibers in 2014
Design	Cross-dispersed echelle spectrograph	
Detector	1k1/2k2 CCD	ELODIE/CORALIE
Sampling	2/3.3	Pixels per FWHM of unresolved line
Spectral domain	383–690 nm	
Resolving power R	42,000/50,000(60,000)	ELODIE/CORALIE (after upgrade 2007)
Total efficiency	1.5%/1.5%(6%)	ELODIE/CORALIE (after upgrade 2007)
RV precision	15/7(3) m s^{-1}	ELODIE/CORALIE (after upgrade 2014)

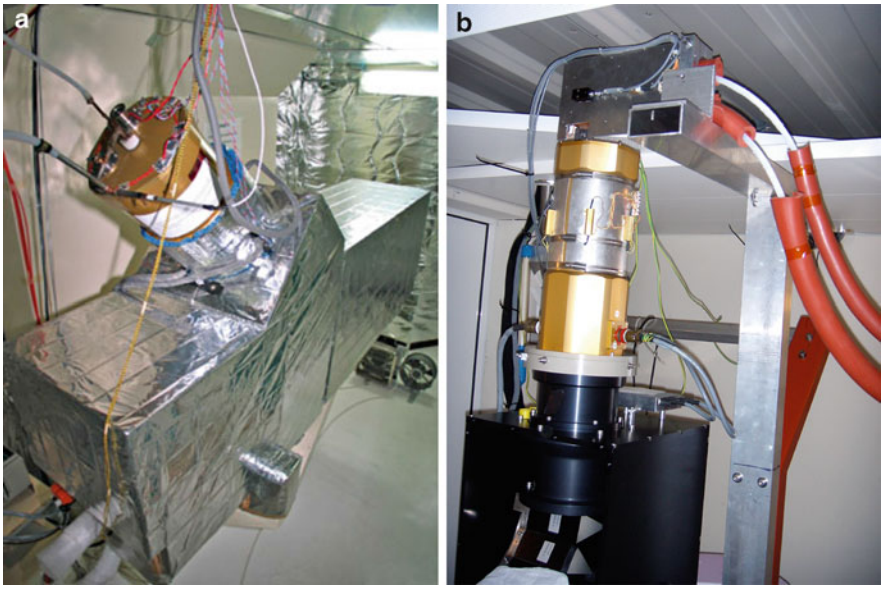

Fig. 3 Left: Picture of the ELODIE spectrograph. Right: Prisms-based cross-disperser of CORALIE after the 2007 upgrade

Soon after the discovery of 51 Peg b, an improved copy of the instrument, named CORALIE, was built for the 1.2-m Euler Swiss Telescope of the ESO-La Silla Observatory (Chile). The CORALIE front-end adaptor is located at the Nasmyth focus of the Euler telescope. A set of two fibers feeds the spectrograph that is located in an isolated and temperature controlled room. Thanks to a slightly

different optical combination at the entrance of the spectrograph and the use of a 2 k by 2 k CCD detector with smaller pixels (15 microns), CORALIE achieved a larger resolving power ($R = 50{,}000$) than ELODIE. The many improvements carried out in the thermal control and the resolution of the instrument, as well as in the reduction software, yielded a factor two improved radial-velocity precision compared to ELODIE.

Operations of CORALIE started in 1998. Several upgrades were performed on the instrument since then: The original cross-disperser made of a combination of prism and grism was replaced by a single prism in 2007. At the same occasion, the input focal ratio of the beam entering the fiber was adapted and a higher resolving power obtained. In 2014, the fiber link (including the scrambler) was entirely replaced using octagonal fibers. All these upgrades helped considerably improving the optical efficiency (by a factor of 4!) and the instrumental precision (from typically 6 to 3 ms^{-1}). In 2015, CORALIE was eventually equipped with a Fabry-Pérot calibrator that allows replacing the thorium lamp in the simultaneous-reference process.

Science Programmes and Results with ELODIE and CORALIE

A radial-velocity survey for northern extrasolar planets led by M. Mayor was conducted from 1994 to 2004 on ELODIE. After the success of the detection of 51 Peg b (Mayor and Queloz 1995), the sample of solar-type stars originally including 142 stars was progressively extended to 372 stars (Perrier et al. 2003). In total, 19 exoplanets were found as part of this early programme, including the planet found to be also transiting HD 209458 (Charbonneau et al. 2000; Mazeh et al. 2000; Henry et al. 2000). In 2004, a new exoplanet research programme was initiated by S. Udry, targeting metal-rich stars expected to have a higher probability of hosting planets. The aim of this project was to improve the statistical studies of planetary parameters, but also to efficiently detect short-period giant planets, ideal candidates for the detection of photometric transits. The strategy consisted in selecting a sample of 1060 dwarf stars of spectral type F8 to M0 with magnitude $V < 8.5$ and vsini <5 kms^{-1} (Da Silva et al. 2006). This large programme was conducted until the end of ELODIE's operation in 2006. One of its main results was the discovery of the hot Jupiter in transit HD 189733 b (Bouchy et al. 2005) also described in a dedicated Chapter of this Book.

Very early on, the diversity of characteristics presented by the newly discovered planetary systems made clear that existing ideas of planetary formation needed serious revision. Enlarging the number of detected systems was necessary to obtain proper statistical distributions of orbital elements, planetary masses, etc., fundamental for a better understanding of the formation and evolution of these systems. Since the summer of 1998, a large high-precision radial-velocity programme has been carried out with CORALIE. The stars monitored are part of a volume-limited sample of close to 1650 main sequence stars from F8 down to K0 within 50 pc and has a color-dependent distance limit for later-type stars down to M0 with the faintest

target not exceeding V = 10. Observations are still ongoing today. The selection of the sample, as well as early results of the programme, is described in Udry et al. (2000). Over about 2 decades, CORALIE has allowed (or has contributed to) the detection of close to hundred extrasolar planet candidates, with periods ranging from a few days (Udry et al. 2000) to very long periods, over 15 years (Ségransan et al. 2010; Marmier et al. 2013), sometimes on very eccentric orbits (Tamuz et al. 2008). The CORALIE planet-search programme around solar-type stars played a very important role in bringing observational constraints to giant planet formation models through well-defined statistics of giant planet properties, including, e.g., stellar-host metallicity (Santos et al. 2001, 2003, 2004b).

With the increasing popularity of ground-based transit searches, the need for vetting of false positives (mimics due to different astrophysical or noise origins) and for planet candidate confirmation (mass estimate) through radial-velocity measurements increased concurrently. The precision of the CORALIE measurements together with the flexibility and high efficiency of the semiautomatic Euler telescope provide a very powerful instrument for transit follow-up. Well over hundred planet candidates detected by the Super-WASP survey (Pollacco et al. 2006) have been confirmed and weighted with this facility. CORALIE will as well play a major role in the follow-up of transiting candidates from newly started ground-based surveys as, e.g., NGTS (Next Generation Transit Survey; Wheatley et al. 2017) or the TESS space mission (Ricker et al. 2015).

HARPS: Setting New Standards

A Strategic Decision

HARPS was conceived, right from its origins, as a high-precision radial-velocity experiment. It was given as an answer to ESO's Announcement of Opportunity published in June 1998 calling for an instrument making best use of the 3.6-m telescope at the La Silla Observatory and aiming at searching for low-mass extrasolar planets. ESO followed so the general recommendations by ESO's Working Group on the Detection of Extrasolar Planets (Paresce and Renzini 1997), and asked explicitly for an instrument of 1 ms^{-1} precision while promising to dedicate 100 nights per year for a total of 5 years to Guarantee Time Observations (GTO), both precision and time coverage being necessary for a comprehensive – and successful – planet search programme.

Under these constraints, the selected HARPS Consortium.[1] Started first a conceptual study, and then later the detailed design of the new spectrograph. Given the composition of the Consortium and the associated technical experience, and in

[1]The HARPS Consortium was led by the Geneva Observatory (University of Geneva, PI: M. Mayor) and also composed of the Observatoire de Haute-Provence (OHP, F), the Physikalisches Institut der Universität Bern (CH), the Service d'Aéronomie de Paris (F) and the European Southern Observatory (ESO).

order to minimize risks, it appeared natural to start with an ELODIE/CORALIE-based design and adopt the simultaneous reference technique. The guideline was to determine the precision-limiting factors, and either mitigate or totally remove these factors in the new design.

Building on Experience

Tests conducted on the CORALIE spectrograph in 1998 demonstrated that the differential drift measured at the relative motion of the spectra of the two fibers illuminated simultaneously with the same calibration source could be kept as low as 1.8 ms^{-1} *rms*. In 2000, the 1.2-m Swiss Euler telescope was pointed toward the Sun, and CORALIE was used to measure solar p-modes. By binning the measurements, the p-modes are averaged out (see Fig. 4 and Queloz et al. 2011). The measured dispersion of the binned data and their evolution with binning revealed the longer-term precision of the instrument, which, in the case of CORALIE, goes well below the ms^{-1} level.

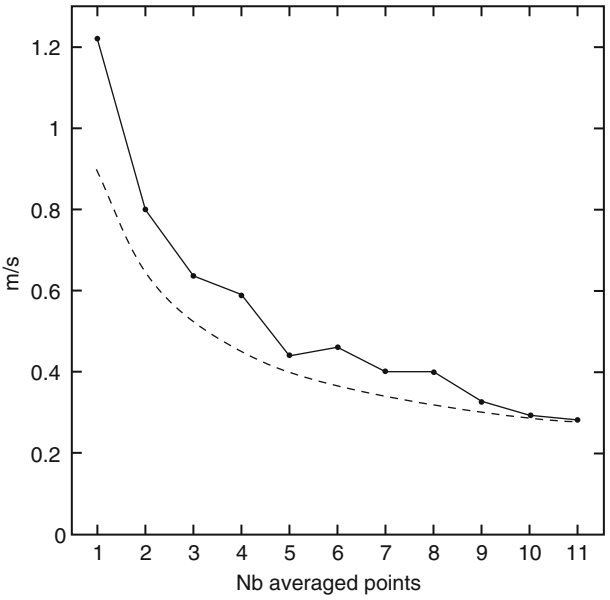

Fig. 4 Original plot of the observed radial-velocity dispersion on a 4-h observation sequence of the Sun from Queloz et al. (2011). The dispersion for different numbers of averaged measurements is displayed, which demonstrates that the Sun oscillations and possible instrumental errors are averaged out. The hatched curve indicates the expected uncertainties on the radial velocity from the photon-noise error on the measurement. With an average of 10 radial-velocity measurements, the dispersion is as low as 0.3 ms^{-1}

These tests demonstrated that, as long as the absolute position of the two spectra on the detector remained within a small fraction of a pixel, the simultaneous reference technique would be able to track possible drifts and correct for them. The indirect implication was, however, that the instrument would have to remain as stable as possible within two calibration sequences (typically 24 h) and that possible larger instabilities of the spectrograph would be "seen" by the absolute wavelength calibration.

However, other tests conducted on CORALIE showed that even fiber-fed spectrographs are sensitive, in terms of radial-velocity precision, to varying slit (or fiber) illumination. The effect was already well known from laboratory tests and simulations (Brown 1990; Avila et al. 1998; Hunter and Ramsey 1992), but they were observed and quantified for stellar observations for the first time with CORALIE (Pepe 2001). Although taken under different conditions, the laboratory and sky measurements of this effect confirmed to be of a similar magnitude but actually at least one order of magnitude too high to be compatible with the 1 ms^{-1} level measurements. Depending on guiding performance and seeing conditions, the varying slit illumination caused effects of up to 5–10 ms^{-1} on CORALIE.

Achieving 1 ms^{-1} Precision

How to achieve 1 ms^{-1} starting from this situation? The very promising results on differential precision were a source of confidence that the design based on the simultaneous reference concept could produce the desired performances. Nevertheless, the identified limitations had to be addressed. The chosen approach was to improve the concept only where needed, but in those cases to go for a "maximum" solution, i.e., choose the solution that would reasonably provide the best guarantees for success within the available constraints of funding and schedule. In particular, the following aspects were addressed:

1. **Intrinsic stability of the spectrograph:** In order to avoid that the spectrum (calibration or stellar) moves on the CCD and produces second-order effects not recorded by the simultaneous reference, the following measures were adopted.
   (a) The whole spectrograph was placed in vacuum. The underlying idea was that the spectrum should not move by more than the equivalent of a few ms^{-1} during a night due to pressure changes, what implied that the air index (or density) should remain stable at the level of 10^{-5} in relative terms. The simplest and most efficient solution to avoid these effects was to keep the air pressure in the spectrograph below 0.01 mbar at any time.
   (b) The temperature of the spectrograph had to be as stable as possible in order to avoid thermomechanical effects. Although the requirement was set to 0.1 K, it was decided that the mK level stability should be aimed at time scales of a night.
   (c) The mechanical design had to be optimized for intrinsic stability and reliability, i.e., no moving parts inside the vacuum vessel; no adjustment mech-

anisms, screws, springs, etc. (alignment only by machining and shimming); materials with high structural stability and low CTE-to-thermal conductivity ratio; use possibly the same materials everywhere; main-dispersion direction chosen to be horizontal and layout of the design symmetric with regard to a plane containing the gravity vector.

2. **Stabilization of the illumination:** It appeared immediately clear that, in the simultaneous reference technique (Brown 1990), the only cause for a differential drift between the stellar and the reference spectrum would arise from a differential and varying illumination of the two fibers. While there is little reason for the calibration light injection to vary either in near field (spatial distribution across the fibre tip) or in far field (angular distribution of the beam injected into the fibre), for the stellar light either guiding errors and seeing, or variations of the pupil illumination (e.g., vignetting) could produce actually both near-field and far-field variations, respectively, on time scales of minutes and hours. For this reason, it appeared mandatory to use a double scrambler (Brown 1990; Baranne et al. 1996) which mitigates, although not fully removes, these illumination effects. From the CORALIE tests (Pepe 2001), it was extrapolated that, in order to reduce these effects to a level below 1 ms^{-1}, it would be necessary to go for a small fiber (a FOV = 1 arcsec on sky and resolving power R > 80,000) and a stable guiding (= centering of the stellar image on the fiber tip) to better than 0.05 arcsec.

3. **High spectral resolution:** The calibration of a spectrograph is performed using sources of spectral reference (emission and absorption) lines of high stability. Knowing the nominal wavelength of the reference, it can be associated with the pixel coordinate of the detector at which the photocenter of the line is recorded. The function describing the relation between the wavelength and the pixel coordinate is called wavelength solution. The quality of the wavelength solution depends also on the detection process and eventually on how precisely a reference line is sampled and reproduced. Supposing unresolved spectral lines, the photocenter of an individual line will be determined with a precision increasing with resolving power. The relation between precision and resolving power has been studied and described in several occasions (Butler et al. 1996; Bouchy et al. 2001; Pepe et al. 2014). This can be intuitively understood in the way that the error on the line position stays, for a fixed number of photons, in relative terms to the line width. Furthermore, given the fact that the "signal" is given by the line depths, it is also natural that the signal increases with resolving power. When increasing the resolving power and ensuring a sufficient pixel sampling of the line, each pixel will furthermore represent a smaller chunk of wavelength. As a consequence, any geometry, extra- and intra-pixel response non-uniformity, charge-transfer effects, etc. will eventually result in a smaller effect in terms of wavelength and thus radial velocity. For all these reasons, HARPS was specified to have a resolving power of at least $R = 80{,}000$ and a minimum sampling (pixels per FWHM of an unresolved spectral line) of

three pixels. This latter requirement resulted from a study (Wildi 1998, private communication) showing that three pixels were needed to preserve at least 90% of the information content.

Design Choices and Design

The design resulting from the previous conceptual considerations is described in Pepe et al. (2002) and Pepe (2001) and the instrument's characteristics summarised in Table 3. HARPS is a *fiber-fed*, cross-dispersed echelle spectrograph using the simultaneous reference technique. The fiber-feed is equipped with a *doubled scrambler* and a guiding-centering system to improve illumination stability. High instrumental stability is achieved by optimizing the thermomechanical design. In particular, the whole spectrograph (all the optics after the fiber feed) is placed in *vacuum*. The optical design is based on the simplest possible *white-pupil mount* (Fig. 5) in totally fixed configuration, i.e., there are *no moving parts*, degrees of freedom were reduced to the absolute necessary minimum, and *no adjustment mechanisms* where allowed (alignment by machining and shimming).

The structure holding the optics is made of welded high-quality carbon steel, thermally cycled and remachined to remove stresses and obtain the desired mechanical accuracy, and is Nickel-plated for protection against corrosion and oxidation. This choice was preferred with regard to Invar and stainless steel because of short- and long-term structural stability, ratio between thermal conductivity and thermal expansion coefficient (more favorable than stainless steel and similar to Invar), simplicity of machining and costs. Other solutions like granite, aluminum, SiC, etc., were considered but discarded because of "risks" of various nature, for instance lack

Table 3 Main characteristics of HARPS/HARPS-N

Parameters	Specification	Comments
Telescope	4-m class	HARPS was installed on the 3–6-m telescope at the ESO-la Silla observatory (1998)
Feed	Fiber-fed spectrograph	Equipped with a double scrambler. HARPS was upgraded to octagonal fibers in may 2015
Design	Cross-dispersed echelle spectrograph	Under vacuum and thermally controlled
Detector	4k4 CCD	Mosaic of two 4k2 CCDs
Sampling (pixels per FWHM)	2/3.3	Pixels per FWHM of unresolved line
Spectral domain	383–690 nm	
Resolving power R	115,000	
Total efficiency	6%(4%)	(HARPS, before upgrade in 2015)
RV precision	0.5–1 m s^{-1}	

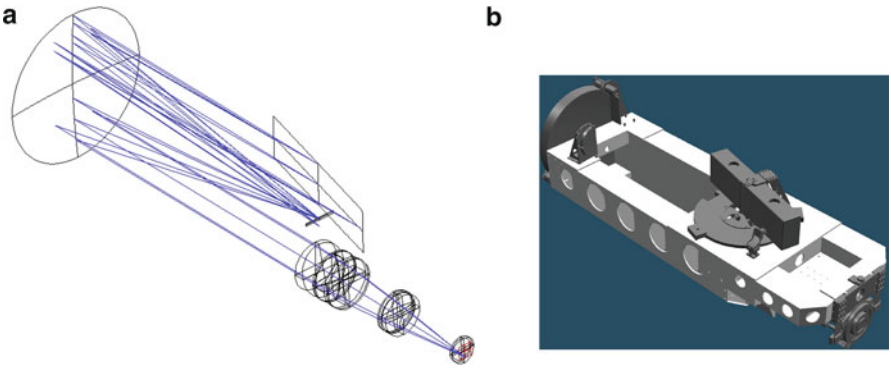

Fig. 5 Isometric view of the optical ray-tracing (left) and of the optomechanical layout of HARPS (right)

of experience and examples, availability and price, complexity of machining, and assembling. This latter point was even more emphasized by the choice of placing the spectrograph in a vertical plane instead of a "table-top" configuration. The whole assembly is mounted thus *fully symmetrically with respect to a plane containing the gravity vector* (the optical axis remains always in this plane). Furthermore, the main dispersion direction (the direction along which the radial velocity is measured) is perpendicular to this plane: Conceptually, the design being symmetric in this direction, any thermal or structural "instability" should have a zero net effect in terms of radial velocity. In the vertical direction, the cross-dispersion direction, the spectrograph would be more sensitive to such effects but they would not result in a radial-velocity effect, at least not at first order.

We have to point out that the "vertical" mechanical layout allowed to mount the echelle grating on its edge (instead of face-up or face-down), which ensured better "stiffness" of the optical axis. This detail became even more important when it was decided to use the largest available "monolithic" R4 echelle gratings available at that time, i.e., the UVES@VLT-like mosaic of 840 × 208 mm. The choice of this grating became necessary to "minimize" the size and thus the costs of the spectrograph given the aimed spectral resolving power and the 1 arcsec field-of-view of the fiber (see Pepe et al. 2002 for the formula relating these quantities). Both parameters do contribute to increase the photonic precision of the radial-velocity measurement and had to be maximized in order to achieve the scientific goals of HARPS. It must be recalled that the use of an image slicer was methodically discarded because of the high risks of introducing Image Profile (IP) distortions at the only location that would not be tracked by the simultaneous reference fiber spectrum.

Cross-dispersion was achieved by a grism, which combined relatively good efficiency and high dispersion. This solution in transmission is again less sensitive to thermomechanical instability and could be designed such that the beam is not deviated, making the spectrograph very compact. The "classical" camera lens produces finally a spectral format perfectly matching the 4k4 detector (mosaic of

Fig. 6 View of the vacuum vessel containing the integrated spectrograph just before final closing. HARPS provided continuous operation from September 2003 to May 2015 without ever being opened

two 2k4 E2V CCDs) for the full 380–690 nm wavelength range and provides an effective sampling of 3.3 pixels. Also, or in particular, because of the thermal sensitivity of the camera focus, a thermal compensation system had to be introduced in the camera design. The aimed thermal stability for the whole spectrograph further contributed to the overall stability of the spectrum on the chip. The detector is mounted inside an ESO standard continuous-flow cryostat that ensures continuous operations and avoids thermal shocks (e.g., in bath cryostat) or vibrations (e.g., in closed-cycle cryocooler).

The spectrograph is installed in a vacuum chamber (Fig. 6) inside the Coudé-West room of the 3.6-m telescope. A triple system of temperature controls and the passive insulation by the vacuum vessel provide mK stability of the spectrograph on timescales of a night and of a few tens of mK over longer timescales. The optical fibers feeding the spectrograph are connected to the HARPS Cassegrain Fiber Adapter located in the Cassegrain cage of the telescope. The adapter provides all the functionalities for acquisition, guiding, and injection of the calibration light that eventually follows exactly the same path as the stellar light.

Last but not least, we have to mention the HARPS data reduction (DRS or pipeline). HARPS had been conceived right from the beginning as an "experiment" or "facility," and the DRS had to be part of this "machinery." A big step had been made from CORAVEL to ELODIE by converting the physical cross-correlation into a numerical cross-correlation. A second big step had to be made: Extraction and reduction had to be improved in order not to lose signal and not to introduce biases. The DRS had to be able to preserve information and determine the average spectral line position with a precision of 1/1000th of the CCD pixel size! Although an excellent level was achieved right at start of operations, it should not be forgotten that a continuous effort of optimization has been conducted over the lifetime of the instrument to always improve the data quality (see, e.g., Lovis and Pepe 2007) and is still continuing (e.g., Coffinet et al. in prep.).

Results and Achievements of HARPS

The first on-sky tests conducted during the instrument's commissioning phase and early GTO period (Mayor et al. 2003) immediately showed that the instrument was delivering the expected efficiency and precision performances. At timescales of a night; on the bright and quiet star alpha Cen B sub-ms^{-1} was demonstrated. The difference to preceding instruments became even more apparent by the "direct" detection of p-modes (RV-modulations seen directly on the RV-timeseries) on several standard G- and K-stars, for which the amplitude and periodicity of the modulation could actually be measured. Still during commissioning, known planetary stars were observed and the radial-velocity curve reproduced with a dispersion of 1.7 ms^{-1}. Less than 1 year after the first light, a first discovery by HARPS of a planet around the star HD 330075 was published (Pepe et al. 2004). The reported dispersion is of 2.0 ms^{-1}, which includes instrumental effects, photon noise, and, of course, possible stellar jitter and potential undetected additional planets, demonstrating a performance never achieved before.

The tipping point was however achieved with the discovery of μ Ara c, a 10.5 $M_{\oplus}$ planet on a 9.6 days orbit (Santos et al. 2004a). This was, together with 55 Cancri e (McArthur et al. 2004), the first "super-Earth" – a planet with mass lower than the mass of Neptune – to be discovered. The planet was actually found by "chance" since the primary purpose of the intensive measurement campaign was to study the stellar parameters through asteroseismologic measurements. Being the measurements reproducible at the ms^{-1} level over long-time scales, the slow variation of the nightly averaged stellar velocities could be reconducted to the presence of an extrasolar planet orbiting the star.

The fabulous result on μ Ara c gave further confidence in the precision of HARPS and paved the path to many other discoveries in the following years. Most of the "super-Earths" discovered by means of the Doppler technique have actually been discovered by HARPS. This led very early to the conclusion that low-mass planets are much more frequent than massive planets: Lovis et al. (2009) reported, after a first analysis of the full HARPS data, that at least 30% of the stars harbor at least one planet. Furthermore, they found more evidence for the fact that low-mass planets are very rarely "single" but rather part of multiplanetary systems. We may mention the examples of HD 69830 (Lovis et al. 2006, a trio of Neptunes), Gl 581 (Udry et al. 2007, two super-Earths and one Neptune), HD 10180 (Lovis et al. 2011, 7 planets in a single system), or HD 40307 (Mayor et al. 2009, 3 super-Earths), but the many results and achievements of HARPS are best summarized in the statistical study by Mayor et al. (2011) and Bonfils et al. (2013). We should not miss to mentioning a few very specific cases of very challenging single planets systems and/or very close-by objects that are particularly suitable for follow-up programs, for instance the controversial Earth-mass planet alpha Cen Bb (Dumusque et al. 2012), the 3.6 Earth-mass planet in the habitable zone of HD 85512 (Pepe et al. 2011), or, more recently, Proxima Centauri b (Anglada-Escudé et al. 2016). In other cases, HARPS was successfully employed to characterize and measure the mass of transiting planets,

for instance CoRoT-7 (Queloz et al. 2009) or GJ 1214 (Charbonneau et al. 2009). Although some of these planets deserve further investigation, either to confirm their Nature or because they are particularly suitable for follow-up measurement with other techniques, they all have in common tiny, ms^{-1}-level signal which could not be detected without the extreme precision of HARPS.

The HARPS concept has been an inspiration for other instruments like SOPHIE (see next section) or its twin in the northern hemisphere, HARPS-N. These instruments together contributed significantly to the search and characterization of extrasolar planets. In addition, they have been the main contributors to the radial-velocity follow-up of planets discovered by the transit technique. HARPS-N, for instance, has significantly contributed in populating the Mass-Radius diagram of low-mass exoplanets with precise mass measurements of candidates previously detected by the Kepler satellite (see for instance Pepe et al. 2013b, Dumusque et al. 2014, Dressing et al. 2015). Another remarkable system is HD 219134, which hosts several super-Earths (Motalebi et al. 2015). After having been first discovered by HARPS-N, subsequent Spitzer observations revealed that the two innermost planets where actually transiting, making HD 219134 the closest system with transiting exoplanets to our Earth.

Finally, it should not be forgotten that the precision of HARPS-N is based on an exquisite spectroscopic fidelity. This latter is actually fundamental for a new branch of the extrasolar planet science: spectroscopy of planetary atmospheres. It has been demonstrated by Wyttenbach et al. (2015, 2017) that ground-based transit spectroscopy of exoplanets with HARPS can attain or even surpass the quality achieved with Hubble at wavelength observable from the ground. Another example is 51 Peg b, from which Martins et al. (2015) have detected the reflected light using HARPS (Table 3).

SOPHIE: An Extension to the Northern Hemisphere

Rationale

Taking into account the limitations of the ELODIE spectrograph (Baranne et al. 1996) and taking benefits from experience gained on HARPS (Pepe et al. 2002; Mayor et al. 2003), the Haute-Provence Observatory (OHP) team undertook in early 2003 the development and building of a new spectrograph called SOPHIE to be operated at the 1.93-m telescope as a northern counterpart of HARPS. The top-level requirements for SOPHIE were to improve the overall optical throughput of ELODIE by a factor of 10, to increase the spectral resolution from 42,000 to 75,000, and to improve long-term spectral stability and radial-velocity precision by a factor of 2 to 3 compared to ELODIE. SOPHIE's first light was achieved in summer 2006. During the first 10 years of operation, continuous improvements of subsystems were done with the goal to reduce any systematic instrumental effect below 2 ms^{-1}.

Table 4 Main characteristics of SOPHIE

Parameters	Specification	Comments
Telescope	2-m class	SOPHIE is installed on the 193 cm telescope at the Haute-Provence Observatory (2006)
Feed	Fiber-fed spectrograph	SOPHIE+ was equipped with octagonal fibers in 2011
Design	Cross-dispersed echelle spectrograph	Dispersive components in a constant pressure tank
Detector	4k2 CCD	
Sampling	2.7/6.7	Pixels per FWHM of unresolved line [HR/HE]
Spectral domain	387–694 nm	
Resolving power R	75′000/39′000	HR/HE
Total efficiency	4.3%/10.4%	HR/HE (at 550 nm)
RV precision	1–2 m s^{-1}	HR

Spectrograph Design

The entire optical design (Perruchot et al. 2008) was oriented to privilege long-term spectral stability and throughput. To minimize the number of separate optical surfaces, and hence increase the mechanical stability, SOPHIE was conceived as a double-pass Schmidt echelle spectrograph, with a single mirror as both collimator and focuser. Parameters are given in Table 4. Light exiting the fiber link (Fig. 7) is collimated by a spherical mirror and, after folding by a plane mirror, comes through the Schmidt chamber where main dispersion is achieved by the R2 echelle grating, while the cross-dispersion is done with a prism in double pass. The dispersed, returned collimated beams are reflected on the folding mirror and are then focused by the spherical mirror to form through a field lens an image of the spectrum on the CCD behind the pierced plane mirror. Apart from thermal precautions, the keypoint for stability is the encapsulation of the dispersive components in a constant pressure tank of dry Nitrogen sealed by the Schmidt plate. This solution stabilizes the air refractive index and thus removes the sensitivity to atmospheric pressure variations. To avoid any gravity effect, the echelle grating grooves and the cryostat are set vertical.

Front End: Starlight is collected at the telescope's focal plane and feed to the spectrograph through an optical fiber link. Two observation modes are available: the High-Efficiency mode (HE) and the High-Resolution mode (HR), to favor high throughput or better radial velocity precision, respectively. Each mode used two fibers: one for the star and the other (located 1.86 arcmin away) for the sky spectrum or simultaneous-reference lamp exposure. The ELODIE front-end was slightly modified during the first year of operation. The atmospheric dispersion correctors were realigned in October 2008. A new guiding system on the fiber entrance was installed in September 2009 achieving a typical accuracy better than

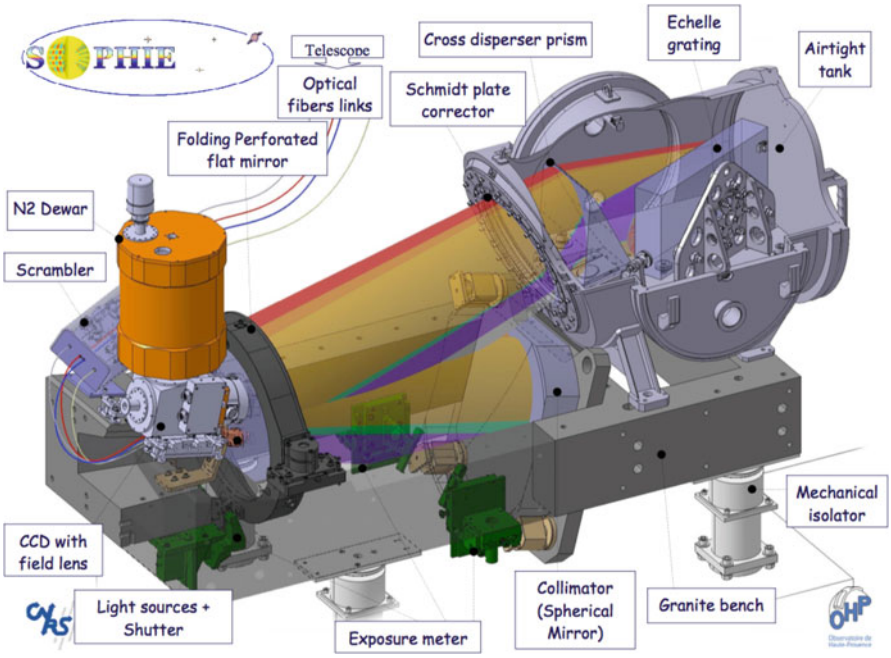

Fig. 7 Design of the SOPHIE spectrograph

0.3 arcsec. The calibration lamps, previously inside the front end, were transferred to a calibration unit in a stabilized environment in fall 2013. All the control hardware of the front end was replaced in spring 2015.

Detector and spectral format: Spectra are recorded by an e2V CCD (4kx2k with 15 μm pixel size) cooled at −100 °C. The detector covers 39 spectral orders for both "star" and "sky" fibers in each mode – HR or HE – from order 50 (680.6 nm to 694.4 nm, dispersion 2.25 Å/mm = 0.034 Å/pixel) to 88 (387.2 nm to 395.5 nm, dispersion 1.27 Å/mm = 0.019 Å/pixel). During the first months of operation, a strong dependency of the radial velocity with the signal-to-noise ratio (SNR) at low flux level was observed, typically below SNR = 70, which corresponds to a flux level of about 600 e^- per pixel. All the spectral lines were blue-shifted at lower flux. Considering that wavelength decreases with increasing distance to the serial register, it was a clear indication for charge transfer inefficiency (CTI). This effect is independent of the used readout mode (slow or fast readout mode). A CTI software correction (Bouchy et al. 2009b) was thus included in the data reduction pipeline of SOPHIE in order to correct for the charge loss during the readout process as a function of pixel coordinate (distance to the register) and flux level.

Back-end environment: The spectrograph is installed in the Coudé room of the 1.93-m telescope building, minimizing the fiber length to 17 m. The whole instrument is mounted on shock absorbers supported by the telescope pillar structure to avoid vibrations. The only moving element, the exposure shutter with an

electromagnetic mechanism, has been cautiously damped to avoid transmission of any vibration through the granite bench. The spectrograph is installed in an isolated and thermally controlled box (itself located inside a two-stage thermalized room at 21 °C) that reduces daily thermal variations to better than 0.01 °C. A continuous LN_2-filing system for CCD cooling at −100 °C was installed in summer 2010 to avoid daily thermal shock and weight change otherwise introduced by the original bath cryostat. A complete upgrade of the thermal control system of the insulated box was performed in spring 2016 in order to reduce the thermal shortcut between optical bench and floor and consequently reduce the residual yearly temperature variations of the instrument.

Optical fiber link: Considering the average seeing on the OHP site of 2.5 arcsec, the field-of-view was chosen to be of 3 arcsec on sky. It is defined by step-index multimode cylindrical optical fibers of 100 μm diameter. To limit focal-ratio degradation (FRD) effects, a compromise is done injecting the light into the fibers at focal ratio f/3.6. A double-scrambler (symmetrical doublets arranged to exchange object and pupil spaces) is included in the HR fiber link to homogenize and to stabilize the spectrograph entrance illumination. In high-resolution (HR) mode, the spectrograph is fed by a 40.5 μm slit bonded to the output of the 100 μm fiber, reaching a spectral resolution of 75,000. In high-efficiency mode (HE), the spectrograph is directly fed by the 100 μm fiber with a resolution power of 39,000. Figure 8 schematically describes the fiber link.

The first years of operation showed that the RV precision obtained on stable stars was limited to 5–6 ms^{-1} in the best cases. This RV limitation was identified as being mainly caused by the insufficient scrambling of the fiber link and the high sensitivity

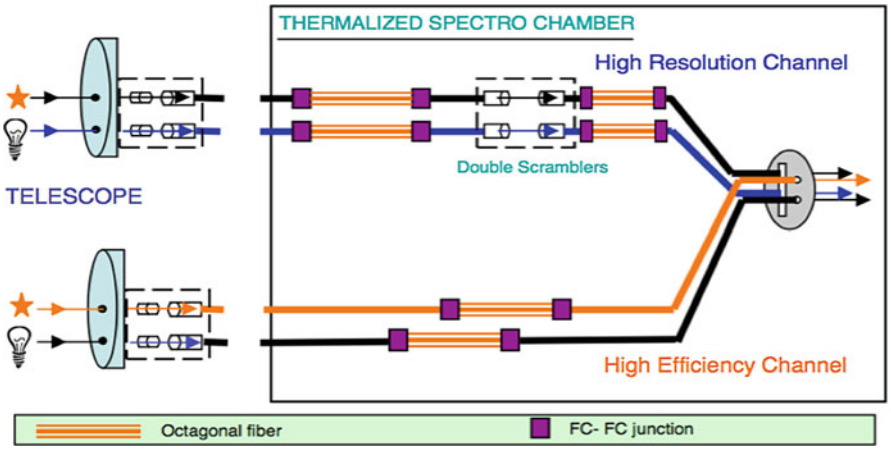

Fig. 8 The SOPHIE fiber-link: It is composed from left to right of: (1) SOPHIE's front-end interface; (2) aperture conversion from f/15 (telescope) to f/3.6 (spectrograph); (3) light transport from the telescope's focal plane to the spectrograph in the Coudé room; (4) light feed of the spectrograph; (5) additional elements for the HR mode (slit and scramblers); and (6) sections of octagonal fiber inserted in 2011 to improve optical scrambling

of the spectrograph to illumination variations. The seeing effect was identified on the HR mode when a correlation was found between the SNR and the radial velocities on several standard stars observed with the same exposure time. This effect, first described by Boisse et al. (2010), appeared to be the limiting factor in SOPHIE's precision. In this regime, when the seeing is improving, mainly the center of the fiber entrance is illuminated. Taking into account the double scrambler, the far field at the fiber output is then mainly illuminated on its central part. Ray-tracing simulations show that the instrumental profile (spot diagrams) depends on the pupil illumination of the spectrograph, and demonstrate that varying illumination of the far field projected on the SOPHIE grating induces pseudo radial-velocity changes that are not symmetric along the spectral orders and therefore introduce a net change in the measured stellar radial velocity. In summary, seeing variations directly translate into radial-velocity changes. To significantly improve the Doppler precision, in summer 2011 octagonal fibers of 1.5 m length were introduced on the paths of fiber A and B of the HR mode upfront the double scrambler. In the HE mode, both fiber A and B were cut and reconnected with a section of octagonal fibers of identical average diameter. The technical details about octagonal fibers, their implementation in the SOPHIE fiber link, as well as first tests are presented by Perruchot et al. (2011) and Bouchy et al. (2013), respectively. The flux loss due to the insertion of octagonal fiber was estimated to be 8% and 10% on fiber A of HR and HE mode, respectively. The SOPHIE spectrograph, with these new octagonal fibers, was renamed to SOPHIE+. The implementation of an octagonal fiber in the fiber link of the SOPHIE spectrograph improved the radial-velocity precision by a factor about 6. In December 2012, 1.5 m-long octagonal fibers were inserted into fiber A and B of the HR mode also *after* of the double scrambler, further improving the illumination stability. The residual limitation of SOPHIE due to its sensitivity to pupil illumination changes is in the current configuration strongly reduced thanks to the octagonal fibers. The typical precision of SOPHIE+ is now in the range 1–2 ms^{-1} on standard solar-type stars observed with the HR+ mode.

Calibration and exposure meter: A tungsten lamp is used to locate the position of the diffraction orders and to measure the flat field. More than one thousand lines of a thorium-argon lamp are used to calibrate the spectra in wavelength with high precision (1–2 ms^{-1}). Each lamp can illuminate both fibers in each mode (HR or HE). Illumination of the sky fiber by the thorium-argon lamp during a stellar exposure (simultaneous-reference technique) allows correcting the residual instrumental drifts. A short-pass rejection filter has been added in April 2007 in front of the lamp to avoid any background caused by wavelengths above 694.6 nm. Furthermore, the simultaneous-reference beam is optically attenuated in the front depending on the exposure time in order to get a constant flux level. The sky fiber can also be used to analyze simultaneously the sky background or the moonlight contamination. An exposure meter records continuously the flux entering the spectrograph. This information is also used to set the optimum observing time depending on atmospheric conditions. Furthermore, the exposure meter allows us to compute the true mean time of the exposures, which is critical for an accurate correction for the Earth's barycentric velocity. In fall 2013, a new calibration

unit was developed and installed in a stable and thermal-controlled environment. This calibration unit included a Laser-Driven Light Source (LDLS) replacing the tungsten lamp, two Thorium-Argon Hollow-Cathode lamps. Finally, a Fabry-Pérot etalon illuminated in white light was added in spring 2017. This Fabry-Pérot replaces the thorium lamp for the simultaneous-reference observations and allows improving the wavelength solution.

Main Science Results

The SOPHIE performances allowed for a dramatic extension of the number of observed stars while pursuing the long-term observations of the ELODIE era (since 1994). SOPHIE plays a very efficient role in the search for northern extrasolar planets including studies on the transition massive planets – brown dwarf (Bouchy et al. 2009a; Diaz et al. 2012), Jupiter analogs (Boisse et al. 2012; Rey et al. 2017), multigiant-planetary systems (Hébrard et al. 2010; Moutou et al. 2014), Neptune-like planet (Courcol et al. 2015), and stellar activity of planetary host stars (Boisse et al. 2009; Aigrain et al. 2012). SOPHIE is also intensively used for the RV follow-up of transit surveys SWASP (Pollacco et al. 2006; Collier Cameron et al. 2007), HAT (Shporer et al. 2009), CoRoT (Barge et al. 2008; Alonso et al. 2008), and Kepler (Santerne et al. 2011; Bouchy et al. 2011a). It led to studies on bloated hot-Jupiter (Hebb et al. 2009; Almenara et al. 2015), Saturn-size planets (Bouchy et al. 2010; Hébrard et al. 2014), misaligned spin-orbit giant planets (Hébrard et al. 2008; Moutou et al. 2009), mass-radius characterization of massive companions in the planet-brown dwarf boundary (Bouchy et al. 2011b; Diaz et al. 2014), and rate of false positive among the Kepler giant candidates (Santerne et al. 2012, 2016).

Conclusions

From CORAVEL to HARPS and SOPHIE, there has been an impressive evolution of technology based on an approach of small steps, every time improvements had become necessary to overcome precision limitations. This approach is continued with the ESPRESSO instrument (Pepe et al. 2013b), which represents the next step of evolution on an 8-m class telescope. In parallel, great effort is being done to adapt the "HARPS-concepts" developed for high-precision visible spectrographs to the near infra-red domain, and to bring a new generation of NIR instruments like CARMENES@Calar Alto, SPIROU@CFHT, and NIRPS@La Silla to the 1 m s^{-1} level of precision.

ESPRESSO and the infrared spectrographs are however an intermediate step to the next level, i.e., precision spectrographs for extremely large telescopes. A phase A study is currently being conducted to propose such an instrument for the European ELT (HIRES Phase A). Looking forward to these future instruments, we finally would like to remind the reader that instrumental and photon-noise precision have to evolve jointly. Instrumental precision should therefore not be sacrificed on the altar of photons.

Acknowledgments This work has been carried out within the frame of the National Centre for Competence in Research PlanetS supported by the SNSF. The authors acknowledge the financial support of the SNSF. The authors would like to thank in the most sincere way all the persons who have contributed through their passionate and competent, but often unapparent, work of administration, management, engineering, technology, programming, etc., to the great scientific success of the described instruments.

References

Aigrain S, Pont F, Zucker S (2012) A simple method to estimate radial velocity variations due to stellar activity using photometry. Mon Not R Astron Soc 419:3147

Almenara JM, Daminai C, Bouchy F et al (2015) SOPHIE velocimetry of Kepler transit candidates. XV. KOI-614b, KOI-206b, and KOI-680b: a massive warm Jupiter orbiting a G0 metallic dwarf and two highly inflated planets with a distant companion around evolved F-type stars. Astron Astrophys 575:71

Alonso R, Auvergne M, Baglin A et al (2008) Transiting exoplanets from the CoRoT space mission. II. CoRoT-Exo-2b: a transiting planet around an active G star. Astron Astrophys 482:L21

Anglada-Escudé G, Amado PJ, Barnes J et al (2016) A terrestrial planet candidate in a temperate orbit around Proxima Centauri. Nature 536(7617):437–440

Avila G, Buzzoni B, Casse M (1998) Fiber characterization and compact scramblers at ESO. Opt Astron Instrum 3355:900–904

Baranne A, Mayor M, Poncet JL (1979) Coravel – a new tool for radial velocity measurements. Vistas Astron 23:279–316

Baranne A, Queloz D, Mayor M et al (1996) ELODIE: a spectrograph for accurate radial velocity measurements. Astron Astrophys Suppl 119:373–390

Barge P, Baglin A, Auvergne M et al (2008) Transiting exoplanets from the CoRoT space mission. I. CoRoT-Exo-1b: a low-density short-period planet around a G0V star. Astron Astrophys 482:L17

Benz W, Mayor M (1981) A new method for determining the rotation of late spectral type stars. Astron Astrophys 93:235

Benz W, Mayor M (1984) Photoelectric rotational velocities of late-type dwarfs. Astron Astrophys 138:183

Boisse I, Moutou C, Vidal-Madjar A et al (2009) Stellar activity of planetary host star HD189733. Astron Astrophys 495:959

Boisse I, Eggenberger A, Santos NC et al (2010) The SOPHIE search for northern extrasolar planets. III. A Jupiter-mass companion around HD 109246. Astron Astrophys 523:88

Boisse I, Pepe F, Perrier C et al (2012) The SOPHIE search for northern extrasolar planets. V. Follow-up of ELODIE candidates: Jupiter-analogs around sun-like stars. Astron Astrophys 545:55

Bonfils X, Delfosse X, Udry S et al (2013) The HARPS search for southern extra-solar planets. XXXI. The M-dwarf sample. Astron Astrophys 549:75

Bouchy F, Pepe F, Queloz D (2001) Fundamental photon noise limit to radial velocity measurements. A&A 374:733–739

Bouchy F, Udry S, Mayor M et al (2005) ELODIE metallicity-biased search for transiting hot Jupiters. II. A very hot Jupiter transiting the bright K star HD 189733. Astron Astrophys 444:L15

Bouchy F, Hébrard G, Udry S et al (2009a) The SOPHIE search for northern extrasolar planets. I. A companion around HD 16760 with mass close to the planet/brown-dwarf transition. Astron Astrophys 505:853

Bouchy F, Isambert J, Lovis C et al (2009b) Charge transfer inefficiency effect for high-precision radial velocity measurements. EAS Publ Ser 37:247–253

Bouchy F, Hebb L, Skillen I et al (2010) WASP-21b: a hot-Saturn exoplanet transiting a thick disc star. Astron Astrophys 519:9

Bouchy F, Bonomo AS, Santerne A et al (2011a) SOPHIE velocimetry of Kepler transit candidates. III. KOI-423b: an 18 M_{Jup} transiting companion around an F7IV star. Astron Astrophys 533:83
Bouchy F, Deleuil M, Guillot T et al (2011b) Transiting exoplanets from the CoRoT space mission. XV. CoRoT-15b: a brown-dwarf transiting companion. Astron Astrophys 525:68
Bouchy F, Diaz R, Hébrard G et al (2013) SOPHIE+: first results of an octagonal-section fiber for high-precision radial velocity measurements. Astron Astrophys 549:49
Brown TM (1990) High precision Doppler measurements via echelle spectroscopy. In: CCDs in astronomy; Proceedings of the conference, 6–8 Sept 1989 (A91-45976 19-33). Astronomical Society of the Pacific, San Francisco/Tucson, pp 335–344
Butler RP, Marcy GW Williams E et al (1996) Attaining Doppler precision of 3 ms^{-1}. Publ Astron Soc Pac 108:500
Campbell B, Walker G (1979) Precision radial velocities with an absorption cell. PASP 91:540
Charbonneau D, Brown TM, Latham DW, Mayor M (2000) Detection of planetary transits across a sun-like star. Astrophys J 529:45
Charbonneau D, Berta ZK, Irwin J et al (2009) A super-earth transiting a nearby low-mass star. Nature 462(7275):891–894
Collier Cameron A, Bouchy F, Hébrard G et al (2007) WASP-1b and WASP-2b: two new transiting exoplanets detected with SuperWASP and SOPHIE. Mon Not R Astron Soc 375:951
Courcol B, Bouchy F, Pepe F et al (2015) The SOPHIE search for northern extrasolar planets. VII. A warm Neptune orbiting HD 164595. Astron Astrophys 581:38
Da Silva R, Udry S, Bouchy F et al (2006) Elodie metallicity-biased search for transiting hot Jupiters. I. Two hot Jupiters orbiting the slightly evolved stars HD 118203 and HD 149143. Astron Astrophys 446:717
Diaz R, Santerne A, Sahlmann J et al (2012) The SOPHIE search for northern extrasolar planets. IV. Massive companions in the planet-brown dwarf boundary. Astron Astrophys 538:113
Diaz RF, Montagnier G, Leconte J et al (2014) SOPHIE velocimetry of Kepler transit candidates. XIII. KOI-189 b and KOI-686 b: two very low-mass stars in long-period orbits. Astron Astrophys 572:109
Dressing C, Charbonneau D, Dumusque X et al (2015) The mass of Kepler-93b and the composition of terrestrial planets. Astrophys J 800(2):7
Dumusque X, Pepe F, Lovis C et al (2012) An earth-mass planet orbiting α Centauri B. Nature 491:207–211
Dumusque X, Bonomo AS, Haywood RD et al (2014) The Kepler-10 planetary system revisited by HARPS-N: a hot rocky world and a solid Neptune-mass planet. Astrophys J 789(2):14
Felgett P (1953) Opt Acta 2:9
Griffin RF (1967) A photoelectric radial-velocity spectrometer. Astrophys J 148:465
Hebb L, Collier-Cameron A, Loeillet B et al (2009) WASP-12b: the hottest transiting extrasolar planet yet discovered. Astrophys J 693:1920
Hébrard G, Bouchy F, Pont F et al (2008) Misaligned spin-orbit in the XO-3 planetary system? Astron Astrophys 488:763
Hébrard G, Bonfils X, Ségransan D et al (2010) The SOPHIE search for northern extrasolar planets. II. A multiple planet system around HD 9446. Astron Astrophys 513:69
Hébrard G, Santerne A, Montagnier G et al (2014) Characterization of the four new transiting planets KOI-188b, KOI-195b, KOI-192b, and KOI-830b. Astron Astrophys 572:93
Henry GW, Marcy G, Butler RP, Vogt S (2000) A transiting "51 Peg-like" planet. Astrophys J 529:41
Hunter TR, Ramsey LW (1992) Scrambling properties of optical fibers and the performance of a double scrambler. Astron Soc Pac 104:1244–1251
Latham DW, Stefanik RP, Mazeh T, Mayor M, Burki G (1989) The unseen companion of HD114762 – a probable brown dwarf. Nature 339:38
Lovis C, Pepe F (2007) A new list of thorium and argon spectral lines in the visible. A&A 468(3):1115–1121
Lovis C et al (2006) An extrasolar planetary system with three Neptune-mass planets. Nature 441:305–309

Lovis C, Mayor M, Bouchy F et al. (2009) Towards the characterization of the hot Neptune/super-Earth population around nearby bright stars. Transiting Planets. Proceedings of the International Astronomical Union, IAU symposium, vol 253, pp 502–505
Lovis C, Ségransan D, Mayor M et al (2011) The HARPS search for southern extra-solar planets. XXVIII. Up to seven planets orbiting HD 10180: probing the architecture of low-mass planetary systems. Astron Astrophys 528:16
Marmier M, Ségransan D, Udry S et al (2013) The CORALIE survey for southern extrasolar planets. XVII. New and updated long period and massive planets. Astron Astrophys 551:A90
Martins JHC, Santos N, Figueira P et al (2015) Evidence for a spectroscopic direct detection of reflected light from 51 Pegasi b. Astron Astrophys 576:9
Mayor M (1980) Metal abundance of F and G dwarfs determined by the radial velocity scanner CORAVEL. Astron Astrophys 87:1
Mayor M, Queloz D (1995) A Jupiter-mass companion to a solar-type star. Nature 378(6555): 355–359
Mayor M, Pepe F, Queloz D et al (2003) Setting new standards with HARPS. The Messenger (ISSN0722–6691) 114:20–24
Mayor M, Udry S, Lovis C et al (2009) The HARPS search for southern extra-solar planets. XIII a planetary system with 3 super-earths (4.2, 6.9 and 9.3 Mearths). Astron Astrophys 493(2): 639–644
Mayor M, Marmier M, Lovis C et al (2011) The HARPS search for southern extra-solar planets XXXIV. Occurrence, mass distribution and orbital properties of super-earths and Neptune-mass planets. arXiv 1109:2497
Mazeh T, Naef D, Torres G, Latham DW et al (2000) The spectroscopic orbit of the planetary companion transiting HD209458. Astrophys J 532:55
McArthur BE, Endl M, Cochran WD et al (2004) Detection of a Neptune-Mass Planet in the ρ Cancri System Using the Hobby-Eberly Telescope. The Astrophysical Journal 614:L81
Motalebi F, Udry S, Gillon M et al (2015) The HARPS-N rocky planet search. I. HD 219134b, a transiting rocky planet in a multi-planet system at 6.5 pc from the sun. Astron Astrophys 584:72
Moutou C, Hébrard G, Bouchy F et al (2009) Photometric and spectroscopic detection of the primary transit of the 111-day-period planet HD 80 606 b Astronomy and Astrophysics 498:L5
Moutou C, Hébrard G, Bouchy F et al (2014) The SOPHIE search for northern extrasolar planets. VI. Three new hot Jupiters in multi-planet extrasolar systems. Astron Astrophys 563:22
Paresce F, Renzini A (1997) The search for extrasolar planets at ESO. The Messenger 90:15–18
Pepe F (2001) HARPS Final design and performance report, ESO Archive 3M6-TRE-HAR-33100-0013, 28 Feb 2001
Pepe F, Mayor M, Rupprecht G et al (2002) HARPS: ESO's coming planet searcher. Chasing exoplanets with the La Silla 3.6-m telescope. The Messenger (ISSN 0722-6691) 110:9–14
Pepe F, Mayor M, Queloz D et al (2004) The HARPS search for southern extra-solar planets. I. HD 330075 b: a new "hot Jupiter". A&A 423:385–389
Pepe F, Cameron AC, Latham DW et al (2013b) An earth-sized planet with an earth-like density. Nature 503(7476):377–380
Pepe F, Lovis C, Ségransan D et al (2013a) The HARPS search for earth-like planets in the habitable zone. I. Very low-mass planets around HD 20794, HD 85512, and HD 192310. Astron Astrophys 534:16
Pepe F, Molar P, Cristiani S et al (2013b) ESPRESSO: the next European exoplanet hunter. Astron Nachr 335(1):8
Pepe F, Ehrenreich D, Meyer M (2014) Instrumentation for the detection and characterization of exoplanets. Nature 513(7518):358–366
Perrier C, Sivan JP, Naef D et al (2003) The ELODIE survey for northern extra-solar planets. I. Six new extra-solar planet candidates. Astron Astrophys 410:1039
Perruchot S, Kohler D, Bouchy F et al (2008) The SOPHIE spectrograph: design and technical key-points for high throughput and high stability. Proc SPIE 7014:12
Perruchot S, Bouchy F, Chazelas B et al (2011) Higher-precision radial velocity measurements with the SOPHIE spectrograph using octagonal-section fibers. Proc SPIE 8151:815115

Pollacco D, Skillen I, Collier Cameron A et al (2006) The WASP project and SuperWASP camera. Astrophys Space Sci 304:253–255

Queloz D, Bouchy F, Moutou C et al (2009) The CoRoT-7 planetary system: two orbiting super-earths. Astron Astrophys 506(1):303–319

Queloz D, Mayor M, Udry S et al (2011) From CORALIE to HARPS. The way towards 1 m s^{-1} precision Doppler measurements. The Messenger (ISSN 0722-6691) 90:15–18

Rey J, Hébrard G, Bouchy F et al (2017) The SOPHIE search for northern extrasolar planets. XII. Three giant planets suitable for astrometric mass determination with Gaia. Astron Astrophys 601:9

Ricker G, Winn J, Vanderspek R, Latham DW, Bakos G et al (2015) Transiting exoplanet survey satellite (TESS). J Astron Telesc Instrum Syst 1:014003

Santerne A, Diaz RF, Bouchy F et al (2011) SOPHIE velocimetry of Kepler transit candidates. II. KOI-428b: a hot Jupiter transiting a subgiant F-star. Astron Astrophys 528:63

Santerne A, Diaz RF, Moutou C et al (2012) SOPHIE velocimetry of Kepler transit candidates. VII. A false-positive rate of 35% for Kepler close-in giant candidates. Astron Astrophys 545:7

Santerne A, Moutou C, Tsantaki M et al (2016) SOPHIE velocimetry of Kepler transit candidates. XVII. Astron Astrophys 587, 64

Santos NC, Israelian G, Mayor M (2001) The metal-rich nature of stars with planets. Astron Astrophys 373:1019

Santos NC, Israelian G, Mayor M, Rebolo R, Udry S (2003) Statistical properties of exoplanets. II. Metallicity, orbital parameters, and space velocities. Astron Astrophys 398:363

Santos NC, Bouchy F, Mayor M et al (2004a) The HARPS survey for southern extra-solar planets II. A 14 earth-masses exoplanet around μ Arae. A&A 426:L19–L23

Santos NC, Israelian G, Mayor M (2004b) Spectroscopic (Fe/H) for 98 extrasolar planet-host stars.Exploring the probability of planetary formation. Astron Astrophys 415:1153

Ségransan D, Udry S, Mayor M et al (2010) The CORALIE survey for southern extrasolar planets. XVI. Discovery of a planetary system around HD147018 and of two long period and massive planets orbiting HD171238 and HD204313. Astron Astrophys 511:A45

Shporer A, Bakos G, Bouchy F et al (2009) HAT-P-9b: a low-density planet transiting a moderately faint F star. Astrophys J 690:1393

Tamuz O, Ségransan D, Udry S et al (2008) The CORALIE survey for southern extra-solar planets. XV. Discovery of two eccentric planets orbiting HD4113 and HD156846. Astron Astrophys 480:33

Udry S, Mayor M, Naef D et al (2000) The CORALIE survey for southern extra-solar planets. II. The short-period planetary companions to HD75289 and HD130322. Astron Astrophys 356:590

Udry S, Bonfils X, Delfosse X et al (2007) The HARPS search for southern extra-solar planets. XI. Super-Earths (5 and 8 M⊕) in a 3-planet system. Astron Astrophys 469(3):L43–L47

Wheatley P, West R, Goad M et al (2017) The Next Generation Transit Survey (NGTS). Mon Not R Astron Soc 469:2361. (in press)

Wyttenbach A, Ehrenreich D, Lovis C et al (2015) Spectrally resolved detection of sodium in the atmosphere of HD 189733b with the HARPS spectrograph. Astron Astrophys 577:13

Wyttenbach A, Lovis C, Ehrenreich D (2017) Hot exoplanet atmospheres resolved with transit spectroscopy (HEARTS). I. Detection of hot neutral sodium at high altitudes on WASP-49b. Astron Astrophys 602:14